

Prediction of ordered structures in the bcc binary systems of Mo, Nb, Ta, and W from first-principles search of approximately 3,000,000 possible configurations

Volker Blum* and Alex Zunger

National Renewable Energy Laboratory, Golden, Colorado 80401, USA

(Received 20 January 2005; published 15 July 2005; publisher error corrected 2 August 2005)

We predict ground states of the refractory alloys Nb-Mo, Nb-W, Ta-Mo, and Ta-W by combining first-principles calculated energies of ≥ 50 configurations for each system with a “mixed-basis cluster expansion,” whose interaction types are chosen with a genetic algorithm search. We find ground states that deviate substantially from the simplified predictions in the literature. These ground states are linked to relatively complex underlying interactions, leading to substantially lower order-disorder transition temperatures than would be expected from simple interaction models, consistent with the extent of the experimentally observed bcc solid solution phases.

DOI: 10.1103/PhysRevB.72.020104

PACS number(s): 61.50.Ah, 61.66.Dk, 81.05.Bx, 81.30.Bx

At low temperatures, all $A_{1-x}B_x$ solid solutions either phase separate or order crystallographically. This choice of phase behavior, as well as the type of ordered structures that emerge from a given alloy system, has long formed the basis for theories of structure and cohesion, and for identifying elemental coordinates (size, electronegativity, valence electron count, orbital radii) that control such behavior.¹⁻⁵ Conversely, such elemental coordinates³⁻⁵ are often used to guess ordering and phase-separation tendencies. Whereas these types of phase behavior are documented for many alloy systems,⁶⁻⁸ in high-melting alloys the slow atomic diffusion at low temperatures often prevents a direct observation of either phase separation or ordering, and only the high-temperature disordered solid solution behavior is observed.⁶⁻⁸ Even so, it is of interest to determine whether the fundamental interatomic interactions are repulsive (leading to positive mixing enthalpies $\Delta H^{(R)} > 0$ for the random alloy, and to eventual phase separation), or attractive (leading to $\Delta H^{(R)} < 0$, and to eventual ordering), for this decides many physical properties even at higher T , including microstructure, transport, and mechanical behavior. Of special interest in this regard are the high-melting (~ 3000 K) refractory binary alloys made of the bcc elements Mo, Nb, Ta, and W, where the observation⁹ of $\Delta H^{(R)} < 0$ suggests ordering, but none was observed as yet⁶⁻⁸ down to the lowest temperatures studied. For the elemental components and heterovalent binary systems, Fig. 1 collects some of the data from which one could attempt to draw a picture of the phase behavior in these systems. We consider first strain-promoting atomic size mismatch (which often discourages lattice ordering²), and charge-transfer-promoting electronegativity differences (which often encourage ordering¹) as well as the d -electron count. We see that the lattice constant mismatch is similar in all cases (~ 0.15 Å), leading to rather small calculated elastic energies (~ 15 meV/atom); the electronegativity mismatch shows no apparent trend with the d -electron count difference. The estimate for mixing enthalpies $\Delta H(x)$ [dashed line in Fig. 1(a)], based on Miedema's³ balance between the atomic size mismatch factor and the charge-mismatch factor, reveals negative ΔH 's with the order $\Delta H(\text{Nb-W}) < \Delta H(\text{Ta-W}) < \Delta H(\text{Nb-Mo}) < \Delta H(\text{Ta-Mo})$, that is almost the reverse of the experimentally observed sequence of $\Delta H^{(R)}$ values⁹ [Fig.

1(a)]. Turning to empirical electronic structure calculations, we find that the tight-binding model of Colinet and Pasturel¹⁰ predicts $\Delta H^{(R)}(\text{Ta-Mo})$ to be below that for $\Delta H^{(R)}(\text{Nb-W})$, the reverse of what Miedema predicts, and in partial opposition to the embedded-atom results of Bangwei *et al.*,¹¹ which show $\Delta H^{(R)}(\text{Nb-W}) > 0$. Figure 1(b) shows the local-density approximation (LDA) calculated formation enthalpies $\Delta H^{(O)}$ for a few selected ordered structures, using the projector-augmented wave method¹² and the exchange-correlation potential of Perdew and Zunger¹³ as implemented in VASP.¹⁴ The overall order of $\Delta H^{(O)}$ is $\Delta H^{(O)}(\text{Ta-Mo}) < \Delta H^{(O)}(\text{Ta-W}) \approx \Delta H^{(O)}(\text{Nb-Mo}) < \Delta H^{(O)}(\text{Nb-W})$, i.e., the opposite of that obtained from the Miedema model. Very recently, Turchi *et al.*^{15,16} studied the phase stability of Mo-Ta-W and its binaries, deriving concentration dependent pair interactions from the single-site coherent potential approximation based on tight-binding linear-muffin-tin-orbital electronic structure calculations in the atomic-sphere approximation. This method neglects (i) the effect of sublattice relaxation, (ii) fluctuations of the alloy environment on the potential and charges at a site, (iii) all three-body and higher multiatom interactions, and (iv) bases its total energies on the sum of eigenvalues only (no electron-electron exchange and Hartree term). Based on only two pair interactions, the *only* predicted ground states of Refs. 15 and 16 are $B2$ (for Mo-Ta and Ta-W), and $D0_3$ (for Ta-W), contradicting, e.g., Fig. 1(b), where the $C11_b$ structure is remarkably stable in addition. Moreover, Turchi *et al.* predict $T_c = 1772$ K for $B2$ Ta-Mo, in contradiction to experiment.⁶⁻⁸ We show below how this overestimation can arise from the use of too simple interactions, placing the quantitative results of Refs. 15 and 16 in serious doubt.

Because the models discussed above do not provide clear answers, we apply the mixed-basis cluster expansion (MBCE) approach¹⁷⁻²⁰ to Nb-Mo, Nb-W, Ta-W, and Ta-Mo.²¹ From a set of LDA calculations for ≥ 50 not necessarily ground-state structures each, we determine for each binary system an Ising-like Hamiltonian that contains (i) a set of long-range pair interactions whose number is *a priori* unlimited,¹⁷ (ii) via a recently developed genetic algorithm,²² the best many-body interactions that are needed both for *fitting* this set of LDA energies, and *predicting* the LDA ener-

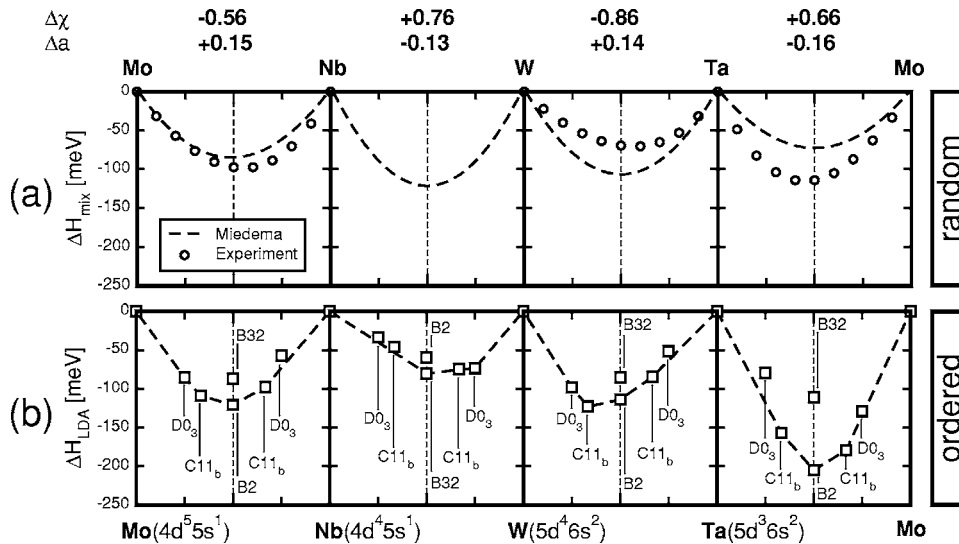


FIG. 1. Fundamental data on the elements Mo, Nb, W, Ta, and their heterovalent binary compounds. The top shows the difference in Pauling electronegativities $\Delta\chi$, and the bcc lattice mismatch Δa (in angstroms) for each binary. (a) The experimental data (Ref. 9) and semiempirical (Miedema) predictions (Ref. 3) for the binary enthalpy of mixing. (b) The LDA-calculated formation enthalpies for simple bcc-based crystal structures.

gies of structures not in the fit, and (iii) strain energies of the long-range elastic limit, via the “constituent strain” term.¹⁷ (i)–(iii) ensure that the number, range, and type of interactions needed to fit and predict LDA energies is determined as objectively as possible. Human subjectivity as to which interactions are needed (e.g., concepts such as “locally complete sets,” (Ref. 23) or cluster variation method aufbau-like hierarchy that forces all subclusters if a given cluster is used²⁴) is avoided. In fact, the interactions that are identified by our approach do not follow any of these *ad hoc* principles. Once a MBCE is available, it can be easily evaluated for each of the 2^N possible binary configurations, producing LDA-quality predictions with errors ≤ 4 meV; in practice, we search²⁵ about 3 000 000 such structures with up to 20 atoms per unit cell. Since the set of LDA input structures is enlarged iteratively while constructing each MBCE,²⁰ the MBCE construction process can also be viewed as an engine that directs us to those candidate ground-state structures that need explicit LDA calculations. The resulting ground-state energetics is shown in Fig. 2(a). For each system, we identify ordered ground-state structures which are not listed in the

established phase diagram collections,^{6–8} unusually low order-disorder transition temperatures, and compositionally asymmetric random alloy mixing enthalpies $\Delta H^{(R)}(x)$.

Ground states of Nb-Mo, Ta-Mo, and Ta-W. These are predicted to have ordered ground states even though none are found in experimental phase diagram collections.^{6–8} Around equiatomic composition, each system is dominated by B2-like structures: The structures Nb₄Mo₃, Nb₄Mo₅, Ta₃W₂, and Ta₃W₄ each contain additional (111) planes of the excess element. However, the ground state at 50% is *not* B2 itself for Nb-Mo and Ta-W, in contrast to earlier predictions.^{15,16,26} Rather, we find the structure labeled B2₃, shown in Fig. 3 together with other key ground states of Mo-Nb, W-Ta, and Ta-Mo. B2₃ is a close relative of the B2 structure, but with an ordered array of antiphase boundaries in every third (110) plane. In the moderately (Mo/W) rich regime, the dominant ground states are regular superlattices of (100) planes [C11_b and “Mo₃Ta₂” (Ref. 21)], whereas the moderately (Nb/Ta) rich regime shows much more complex structures, of the type already predicted for Mo-Ta (Ref. 21) (Mo₄Ta₉, Mo₄Ta₁₂, and Nb₈Mo₄). Any “usual-suspect”

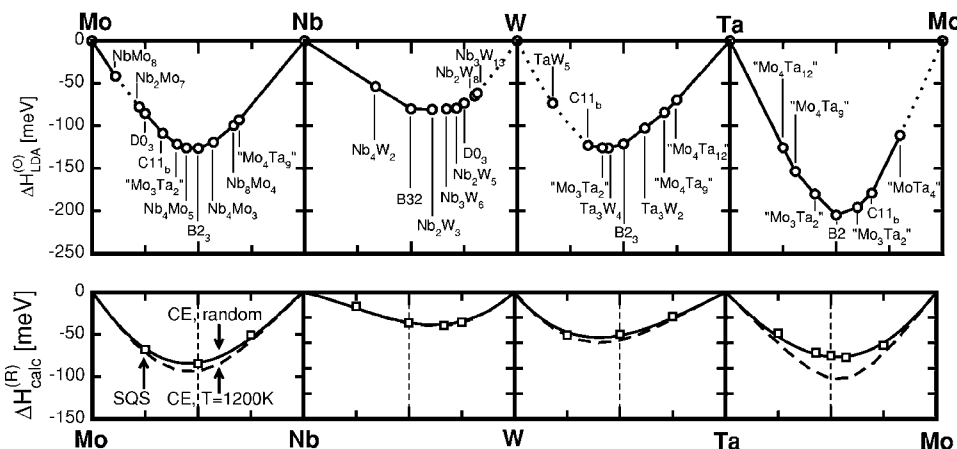


FIG. 2. (a) $\Delta H_{\text{LDA}}^{(O)}$ of predicted ground states out of 3,000,000 possibilities in Nb-Mo, Nb-W, Ta-W, and Ta-Mo. Dashed ground-state line segments indicate that both LDA and MBCE predict ground states, but different structures are energetically too close for an unambiguous assignment. (b) Random alloy enthalpy of mixing (solid lines) and enthalpy of mixing of short-range ordered solid solutions at $T = 1200$ K (dashed lines), predicted by the final MBCEs and confirmed by direct LDA calculations for special quasirandom structures (SQS).

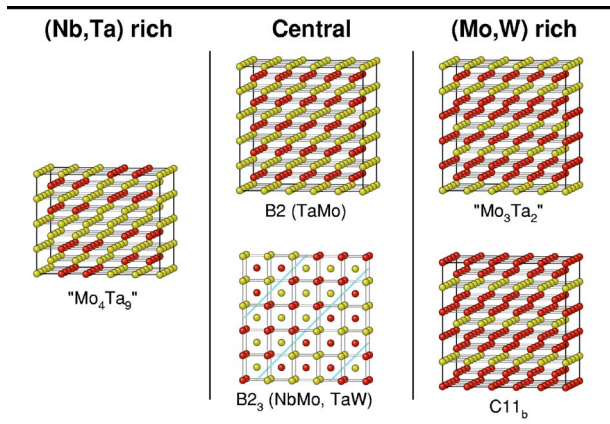


FIG. 3. (Color online) Dominant ground-state structures in the Nb-Mo, Ta-Mo, and Ta-W systems. (110) antiphase boundaries in the $B2_3$ structures are emphasized by blue planes.

ground states are prominently absent on the (Nb/Ta)-rich side. Remarkably, the ground-state line segments of Mo-rich Nb-Mo, W-rich Ta-W, and Mo-rich Ta-Mo are densely decorated by structures on or near the ground-state line. Such dense sequences can arise as “adaptive structures,” (Refs. 27 and 28) where long-ranged competing interactions allow stable structures at immediately adjacent x , creating a continuous convex curve $\Delta H^{(0)}(x)$. In contrast, the dilute (Nb/Ta)-rich regimes, beyond the complex Mo_4Ta_9 -like structures, are devoid of truly stable structures altogether. The complexity of all three ground-state lines shows the need of realistic, first-principles-based interactions whose predictive power is carefully checked. For Mo-Ta and Ta-W, this complexity is missed entirely by the simpler scheme of Turchi *et al.*^{15,16} Very recently, Curtarolo *et al.*²⁹ used a fixed library of 176 different structures within a data-mining³⁰ density functional theory-based series study of binary ground states. They predict for Nb-Mo correctly the Mo-rich $C11_b$ and $D0_3$ structures, but incorrectly the $B2$ and Nb-rich $C11_b$ structures. Our results [Fig. 3(a)] agree with the data-mining approach where the actual ground states

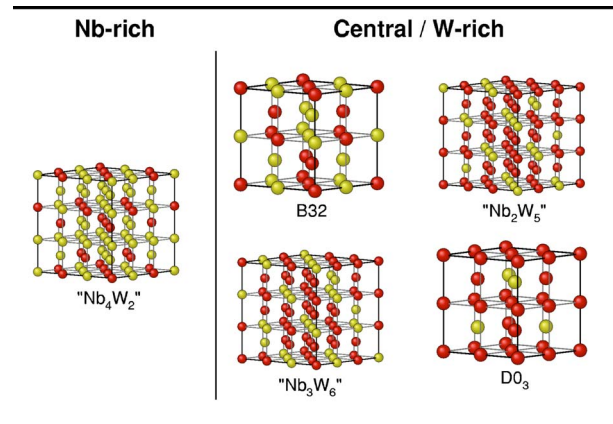


FIG. 4. (Color online) Dominant ground-state structures in the Nb-W system.

happen to be among the 176 preselected structures (Mo-rich $C11_b$ and $D0_3$). However, ground-state configurations such as $B2_3$ and Nb-rich Mo_4Ta_9 are outside any conventional structure library, and will almost inevitably be missed in a prediction scheme based on human-compiled structure lists.

Ground states of Nb-W. The ordering behavior of Nb-W is completely different from the other three systems, despite qualitative indicators that would have suggested similarities (e.g., the close proximity in the periodic system of elements, similar $\Delta\chi$ and lattice mismatch). The key ground state structures of Nb-W are illustrated in Fig. 4. The central ground state (NbW) is $B32$ (the NaTl structure), the A_2B_2 superlattice of (111) atomic planes. In the moderately W-rich range, the appearance of (111) superlattices continues up to the $D0_3$ structure [the A_3B (111) superlattice], with hybrid superlattices of longer period in between ($\text{Nb}_2\text{W}_3, \text{Nb}_3\text{W}_6, \text{Nb}_2\text{W}_5$). Qualitatively, these structures form a remarkable contrast to the (100)-like features of the other three systems. Above 75% W, the sequence of (111) superlattices is replaced by a dense succession of structures on or near the ground-state line (dashed region), first by defective versions of the $D0_3$ structure, and finally by larger-cell dilute structures. The Nb-rich side shows only one shal-

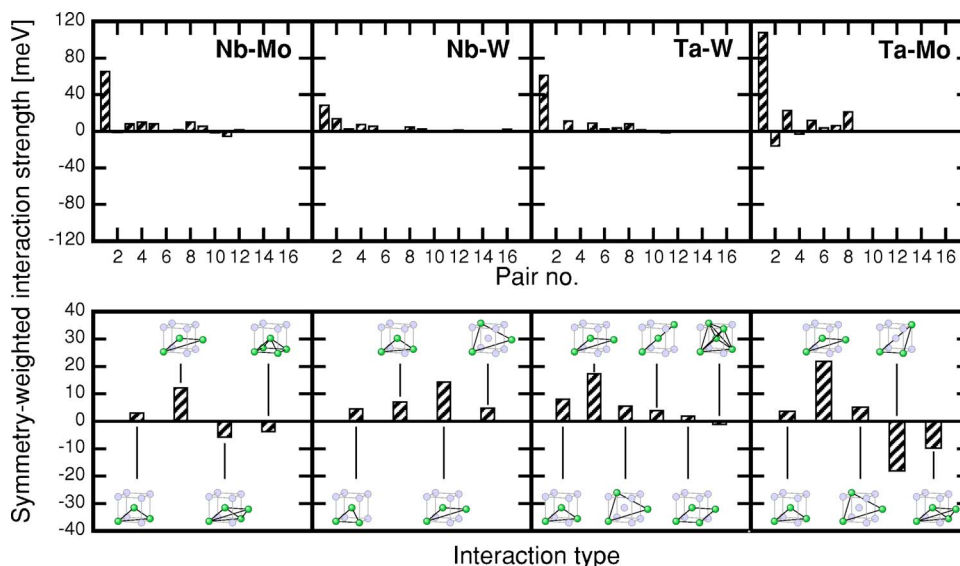


FIG. 5. (Color online) Automatically selected symmetry-weighted pair and many-body interactions for the MBCEs of Nb-Mo, Nb-W, Ta-W, and Ta-Mo.

TABLE I. Critical temperatures (in K) of order-disorder transitions at equiatomic composition ($x=50\%$) in Nb-Mo, Nb-W, Ta-W, and Ta-Mo from the present paper, simplified theoretical predictions in the literature and simplified model energetics based on the six shortest-ranged bcc interactions and the structures in Fig. 1(b).

Energetics	Nb-Mo	Nb-W	Ta-W	Ta-Mo
Converged MBCE	540	320	360	800±200 (Ref. 20)
Literature (Ref. 26)	800		920	1040
Literature (Ref. 15 and 16)			1000	1772
Simplified CE	910	460	740	1800

low ground-state structure in LDA (Nb_4W_2), which is in principle the $B32$ structure, but with pure Nb (100) planes inserted after every second plane.

All pair and many-body interactions are shown in Fig. 5. The difference between Nb-W and the other three systems is found in the smaller pairs beyond the first-nearest-neighbor interaction (which is always attractive). In contrast, three of the four many-body figures that characterize Nb-W are also found for Ta-W and Ta-Mo, and their relative magnitude is even quantitatively similar between the three systems. Figure 2(b) shows the calculated energy of ideally random ($T \rightarrow \infty$) solid solutions, $\Delta H^{(R)}(x)$ (solid line), and that of short-range ordered solid solutions at $T=1200$ K, $\Delta H^{(\text{SRO})}(x)$ (dashed line). The shape of each calculated curve is confirmed quan-

tatively by direct LDA calculations, using large-cell special quasirandom structures^{20,31} [Fig. 2(b)]. We use canonical Monte Carlo simulations³² to calculate order-disorder transition temperatures at a fixed concentration x (Table I for equiatomic compounds). All predicted T_c lie well below 1000 K, with $T_c^{\text{max}} \approx 600-1000$ K for the $A2-B2$ transition in TaMo.²⁰ T_c 's for $A2-B2$ transitions in Nb-Mo, Ta-W, and Ta-Mo have been predicted before,^{15,16,26} but for much simpler interactions. These predictions (also given in Table I) lie substantially higher than ours, and would place all three T_c in an experimentally accessible range. The overestimation of T_c in Refs. 15, 16, and 26 is caused by the use of simple interactions. We demonstrate this by analyzing restricted cluster expansions with interactions spanning no more than second nearest-neighbor distances, fitted to reproduce only $\Delta H_{\text{LDA}}^{(O)}$ of the $D0_3$, $B32$, and $B2$ structures. The corresponding values of T_c (the third line of Table I) are uniformly larger than those of the full MBCEs, and would contradict the experimental phase diagrams at least for Nb-Mo and Ta-Mo.

In summary, we find that complex ground-state structures coexist with, or even replace, well-known ground-state candidate structures such as $B2$, $B32$, or $C11_b$ in the bcc systems Nb-Mo, Nb-W, Ta-W, and Ta-Mo. The complexity of ground states is directly linked to relatively complex interactions, explaining the experimental observation of extended bcc solid solutions in all four systems despite significantly negative formation enthalpies.

This work was supported by DOE-SC-BES-DMS.

*Present address: Abteilung Theorie, Fritz-Haber-Institut der Max-Planck-Gesellschaft, Faradayweg 4-6, 14195 Berlin-Dahlem, Germany.

¹L. Pauling, *The Nature of the Chemical Bond* (Cornell University Press, Ithaca, 1960).

²W. Hume-Rothery and G. Raynor, *The Structure of Metals and Alloys* (Institute of Metals, London, 1954).

³A. Miedema, *Philips Tech. Rev.* **36**, 217 (1976).

⁴A. Zunger, *Phys. Rev. B* **22**, 5839 (1980).

⁵P. Villars, *J. Less-Common Met.* **92**, 215 (1983); **99**, 33 (1984); **102**, 199 (1984).

⁶R. Hultgren *et al.*, *Selected Values of the Thermodynamic Properties of Binary Alloys* (American Society of Metals, Metals Park, OH, 1973).

⁷*Pearson's Handbook of Crystallographic Data for Intermetallic Phases*, 2nd ed. edited by P. Villars and L. Calvert (ASM International, Materials Park, OH, 1991).

⁸*Phase Equilibria, Crystallographic and Thermodynamic Data of Binary Alloys*, edited by B. Predel, Landolt-Börnstein, New Series, Group IV Vol. 5H (Springer, Berlin, 1997).

⁹S. Singhal and W. Worrell, in *Metallurgical Chemistry*, edited by O. Kubaschewski (Her Majesty's Stationary Office, London, 1974), pp. 65; *Metall. Trans.* **4**, 1125 (1973); **4**, 895 (1973).

¹⁰C. Colinet and A. Pasturel, *Physica B* **159**, 275 (1989).

¹¹Zhang Bangwei and Ouyang Yifang, *Phys. Rev. B* **48**, 3022 (1993).

¹²P. E. Blöchl, *Phys. Rev. B* **50**, 17953 (1994); G. Kresse and D.

Joubert, *ibid.* **59**, 1758 (1999).

¹³J. P. Perdew and A. Zunger, *Phys. Rev. B* **23**, 5048 (1981).

¹⁴G. Kresse and J. Furthmüller, *Phys. Rev. B* **54**, 11169 (1996); *Comput. Mater. Sci.* **6**, 15 (1996).

¹⁵P. E. A. Turchi *et al.*, *Phys. Rev. B* **64**, 085112 (2001).

¹⁶P. E. A. Turchi *et al.*, *Phys. Rev. B* **71**, 094206 (2005).

¹⁷D. B. Laks *et al.*, *Phys. Rev. B* **46**, 12587 (1992).

¹⁸A. Zunger, in *Statics and Dynamics of Alloy Phase Transformations*, edited by P. E. A. Turchi and A. Gonis (Plenum Press, New York, 1994), pp. 361-419.

¹⁹A. Zunger *et al.*, *Modell. Simul. Mater. Sci. Eng.* **10**, 1 (2002).

²⁰V. Blum and A. Zunger, *Phys. Rev. B* **70**, 155108 (2004).

²¹V. Blum and A. Zunger, *Phys. Rev. B* **69**, 020103(R) (2004).

²²G. Hart *et al.* *Nat. Mater.* **4**, 391 (2005).

²³N. A. Zarkevich and D. D. Johnson, *Phys. Rev. Lett.* **92**, 255702 (2004).

²⁴M. Sluiter and Y. Kawazoe, *Phys. Rev. B* **71**, 212201 (2005); M. Sluiter *et al.*, *ibid.* **53**, 6137 (1996).

²⁵L. G. Ferreira *et al.*, *Int. J. Supercomput. Appl.* **5**, 34 (1991).

²⁶C. Sigli and J. Sanchez, *Acta Metall.* **36**, 367 (1988).

²⁷M. Sanati *et al.*, *Phys. Rev. Lett.* **90**, 045502 (2003).

²⁸R. Drautz *et al.*, *Phys. Rev. Lett.* **93**, 067202 (2004).

²⁹S. Curtarolo *et al.*, CALPHAD (2005) in press.

³⁰S. Curtarolo *et al.*, *Phys. Rev. Lett.* **91**, 135503 (2003).

³¹A. Zunger *et al.*, *Phys. Rev. Lett.* **65**, 353 (1990).

³²Z.-W. Lu *et al.*, *Phys. Rev. B* **50**, 6642 (1994).